to ascertain. The decay-associated emission spectra of the two conformers are almost identical. Thus, we do not expect large differences in internal conversion and intersystem crossing rates between conformers. Furthermore, we can estimate the intersystem crossing rate k_{isc} from the temperature-independent rate k_o and the radiative rate k_r, where $k_o = k_r + k_{isc}$. Using data from Table VI [neglecting the nonlinear fit for τ_1 of W(1)E] and radiative rates calculated from quantum yields and mean lifetimes,[59] we obtain intersystem crossing rates of $\sim 5 \times 10^7$ s^{-1} for W(1) and W(1)E. Clearly, small changes in intersystem crossing rate would not account for the difference in lifetimes between conformers. Finally, the Arrhenius data argue that electron transfer is also occurring. The rate of transfer is expected to depend upon distance and perhaps also orientation of the carboxylate relative to the indole ring. It is satisfying that the shorter lifetime component can be associated with the conformer whose carboxylate is nearer the ring. Since the through-bond distance is the same in both conformers, the different lifetimes imply that the electron transfer is through-space. To better our understanding of quenching mechanisms in indole and tryptophan we are currently investigating solvent isotope effects in W(1) and related compounds.

Acknowledgment. We thank Dr. Marco A. Vela for chemical synthesis and HPLC and Dr. Mark L. McLaughlin for helpful discussion. This work was supported by NIH Grants GM35009 and GM42101.

Registry No. W(1), 42438-90-4; W(1)·H_2O, 129848-94-8; W(1)E, 129848-93-7.

Supplementary Material Available: Tables of (I) bond distances, (II) coordinates for hydrogen atoms, (III) bond distances involving hydrogen atoms, (IV) bond angles involving hydrogen, (V) torsion angles, (VI) anisotropic thermal parameters, (VIII) atomic point charges from 3-21G, (IX) defined force constants for atom types assigned in Figure S1, and (X) statistical comparison between geometric parameters of global minimum MM2 and X-ray structures of W(1) zwitterion (12 pages); listing of structure factor amplitudes (×10) (8 pages). Ordering information is given on any current masthead page.

Electron-Rich Iridium Complexes with Mixed-Donor Polydentate Ligands. Chemoselective Catalysts in Hydrogen-Transfer Reduction of α,β-Unsaturated Ketones

Claudio Bianchini,*,† Erica Farnetti,‡ Mauro Graziani,*,‡ Giorgio Nardin,‡ Alberto Vacca,† and Fabrizio Zanobini†

Contribution from the Dipartimento di Scienze Chimiche, Università di Trieste, Piazzale Europa 1, 34126 Trieste, Italy, and Istituto per lo Studio della Stereochimica ed Energetica dei Composti di Coordinazione del CNR, Via J. Nardi 39, 50132 Firenze, Italy.
Received April 30, 1990

Abstract: The mixed-donor polydentate ligands Pr^n-$N(CH_2CH_2PPh_2)_2$ (PNP) and $Et_2NCH_2CH_2N(CH_2CH_2PPh_2)_2$ (P_2N_2) react in THF with $[Ir(cod)(OMe)]_2$ (cod = cycloocta-1,5-diene) yielding the σ,η^2-cyclooctenyl complexes $[(PNP)Ir(\sigma,\eta^2\text{-}C_8H_{13})]$ (**1**) and $[(P_2N_2)Ir(\sigma,\eta^2\text{-}C_8H_{13})]$ (**2**). The crystal structure of **1** has been determined by X-ray methods. The iridium atom is coordinated to the phosphorus and nitrogen donors of PNP and to a cyclooctenyl group via σ and η bonding in a distorted trigonal-bipyramidal geometry. The same coordination geometry is assigned to the P_2N_2 derivative that exhibits a free diethylamino group. In solution, above ca. −30 °C, compounds **1** and **2** are in equilibrium with the hydride η^4-cod isomers $[(PNP)IrH(\eta^4\text{-cod})]$ (**3**) and $[(P_2N_2)IrH(\eta^4\text{-cod})]$ (**4**) via a β-H elimination/hydride migration pathway. The equilibrium constants for the **1** ⇄ **3** and **2** ⇄ **4** interconversions have been obtained at different temperatures by ^{31}P NMR integration in the range 298–348 K. The thermodynamic functions $\Delta H°$ and $\Delta S°$ for the **1** ⇄ **3** and **2** ⇄ **4** isomerization reactions have been calculated. They are rather similar with each other, but the enthalpy contribution appears slightly more favorable for the latter reaction, in nice accord with the higher concentration of the hydride species observed for the P_2N_2 system at comparable temperatures. Compounds **1** and **2** are good catalyst precursors for the chemoselective hydrogen-transfer reduction of α,β-unsaturated ketones such as benzylideneacetone to allylic alcohols. The catalytic activity of **1** and **2** has been compared and contrasted to that exhibited by the system "$[Ir(cod)(OMe)]_2$ + PNP or P_2N_2" prepared in situ as well as other related complexes like $[(PNP)Ir(\eta^4\text{-cod})]BPh_4$ (**5**), $[(P_2N_2)Ir(\eta^4\text{-cod})]BPh_4$ (**6**), $[(triphos)Ir(\sigma,\eta^2\text{-}C_8H_{13})]$ (**7**) and $[(triphos)Ir(\sigma,\eta^2\text{-}C_8H_{13})]BPh_4$ (**8**) [triphos = $MeC(CH_2PPh_2)_3$]. Through this comparison, valuable mechanistic information on the catalysis cycle has been obtained.

High electron density at the metal center seems to be an essential requisite for catalysts capable of selectively reducing α,β-unsaturated ketones to unsaturated alcohols via hydrogen transfer. In particular, the chemoselectivity has been related to the ability of electron-rich metal species to form M–H bonds exhibiting remarkable hydridic character.[1] As a matter of fact, it is not incidental that iridium and tertiary phosphines contribute the essential ingredients in several catalysis systems for such reactions.[2] A particular role appears to be played by bidentate, mixed N, P-donor ligands like Ph_2P-o-C_6H_4-NR_2, as they are known to form excellent iridium catalysts for the chemoselective reduction of α,β-unsaturated ketones.[3] The combination of soft and hard donor atoms, as it occurs in aminophosphine ligands, attracted our attention. In fact, one cannot exclude a priori that free coordination sites may be provided during the catalysis cycle

† ISSECC, CNR.
‡ University of Trieste.

(1) Nakano, T.; Umano, S.; Kino, Y.; Ishii, Y.; Ogano, M. *J. Org. Chem.* **1988**, *53*, 3752.
(2) Rauchfuss, T. B.; Roudhill, D. M. *J. Am. Chem. Soc.* **1974**, *96*, 3098.
(3) Farnetti, E.; Nardin, G.; Graziani, M. *J. Chem. Soc., Chem. Commun.* **1989**, 1264.

0002-7863/90/1512-9190$02.50/0

by the alternative decoordination of either phosphorus or nitrogen donor depending on the formal oxidation state of the metal along the reaction pathway. Certainly, the presence of amine groups does not provide the metal with an extraordinary electron density, especially as compared to ligands containing only phosphorus donors. We therefore decided to investigate the coordinating behavior toward iridium of polydentate ligands where the number of phosphorus donors prevails over that of nitrogen donors. Such polydentate ligands, particularly those having more than three donor atoms, would offer further advantages over mono- or bidentate ligands.[4] Indeed, a polydentate ligand contributes a higher nucleophilicity to the metal and a better control on the stereochemistry and stoichiomery of the resulting complexes.

Two molecules that appear as appropriately designed to combine the *polydentate ligand advantages* with the presence of both phosphorus and nitrogen donors are the potentially tridentate and tetradentate ligands Pr^n-$N(CH_2CH_2PPh_2)_2$ [N,N-bis(2-(diphenylphosphino)ethyl)-*n*-propylamine, PNP][2] and $Et_2NCH_2CH_2N(CH_2CH_2PPh_2)_2$ [N,N-bis(2-(diphenylphosphino)ethyl)-N-(2-(diethylamino)ethyl)amine, P_2N_2]. Both

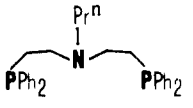

PNP

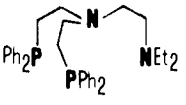

N_2P_2

of them were synthesized in the early seventies by Sacconi and Morassi.[5,6] However, their coordination chemistry has been inadequately studied; only a few examples of cobalt(II) and nickel(II) complexes have been described so far, and no crystal structures are available for PNP complexes.[6] On the basis of UV–vis spectra, the tridentate ligand has been suggested to bind to the metal either in a planar fashion having trans-disposed phosphorus donors (meridional capping) or in a tripodal fashion having cis-disposed phosphorus donors (face capping).[6,7] PNP can behave as a bidentate ligand via decoordination of the nitrogen donor atom. The tripodal ligand P_2N_2 displays a wider bonding capability: bidentate through the phosphorus donors, tridentate through the two phosphorus and the central nitrogen, tetradentate when all of the donor atoms coordinate to the metal.[5,6a,8]

In this paper we report the first pieces of organometallic chemistry and homogeneous catalysis made accessible by the coordination of the PNP and P_2N_2 ligands in iridium. In particular, we describe the reactions of $[Ir(cod)(OMe)]_2$ with PNP and P_2N_2 to give $(\sigma,\eta^2\text{-}C_8H_{13})Ir$[1] complexes which show good selectivity in hydrogen-transfer reduction of α,β-unsaturated ketones to allylic alcohols (cod = cycloocta-1,5-diene). The use of polydentate ligands has allowed us to understand much of the solution chemistry of the catalyst precursors and to propose a reliable catalysis cycle as well.

Experimental Section

General Data. All the reactions and manipulations were routinely performed under a nitrogen atmosphere with standard Schlenk-tube techniques. The complexes $[Ir(cod)(OMe)]_2$[9] and $[Ir(cod)Cl]_2$[10] and the ligands PNP,[5] N_2P_2,[6] and triphos[11] were prepared as described in the literature. Benzylideneacetone was recrystallized three times from propan-2-ol before use. All the other chemicals were reagent grade and were used as received by commercial suppliers. Tetrahydrofuran, THF, was purified by distillation over $LiAlH_4$ under nitrogen just prior to use. Toluene and *n*-pentane were dried over sodium before being purified by distillation under a nitrogen atmosphere. Propan-2-ol and cyclopentanol were distilled over CaO. Infrared spectra were recorded on a Perkin-Elmer 1600 Series FTIR with use of samples mulled in Nujol between KBr plates. Proton NMR spectra were recorded at 299.945 MHz on a Varian VXR 300 spectrometer. ^1H chemical shifts were reported relative to tetramethylsilane as external reference. $^{31}P\{^1H\}$ NMR spectra were recorded on a Varian VXR 300 spectrometer operating at 121.42 MHz. Chemical shifts were relative to external H_3PO_4 85% with downfield values reported as positive. Two-dimensional NMR spectra were recorded by using the VARIAN program COSY with optimized window functions. Conductivities were measured with a WTW Model LBR/B conductivity bridge. THe conductivity data were obtained at sample concentrations of ca. 10^{-3} M in nitroethane solutions. GC analyses were performed on a Shimadzu GC-8A gas chromatograph fitted with a thermal conductivity detector and a 10-ft $^1/_8$ in. SS 10% SP-2100 100/120 Supelcoport column. Formaldehyde was detected as formaldehyde oxazolidine by using a 10% UCON 50 HB-5100/2% KOH on 80/100 Chromosorb W AW, 2 m × 2 mm i.d. glass column. Quantification was achieved with a Shimadzu C-R6A Chromatopac coupled with the chromatograph, operating with an automatic correct area normalization method. The simulation of the $^{31}P\{^1H\}$ spectra was carried out by using an updated version of the LAOCN4 program.[12] The initial choices of shifts and coupling constants were refined by successive iterations, the assignment of the experimental lines being performed automatically. The final parameters gave a fit to the observed line positions better than 0.3 Hz. The catalytic reactions were monitored by glc on a Perkin-Elmer Sigma 3B instrument, using a Supelcowax 10 wide-bore capillary column (30 m × 0.75 mm i.d.).

Synthesis of the Complexes. The solid compounds were collected on sintered-glass frits and washed, unless otherwise stated, with ethanol and *n*-pentane before being dried in a stream of nitrogen.

Preparation of $[(PNP)Ir(\sigma,\eta^2\text{-}C_8H_{13})]$ (1). Solid PNP (0.48 g, 1.0 mmol) was added with stirring to a solution of $[Ir(cod)(OCH_3)]_2$ (0.33 g, 0.50 mmol) in THF (30 mL) at room temperature. Addition of ethanol (30 mL) to the resulting pale yellow solution gave crystals of **1**. Yield 90%. The formation of formaldehyde in the course of the reaction was detected by GC and chemically confirmed by the dimedone method.[13] Anal. Calcd for $C_{39}H_{48}IrNP_2$: C, 59.67; H, 6.16; N, 1.78; Ir, 24.49. Found: C, 59.46; H, 6.08; N, 1.64; Ir, 24.31.

Preparation of $[(P_2N_2)Ir(\sigma,\eta^2\text{-}C_8H_{13})]$ (2). Compound **2** was prepared as described above by using P_2N_2 (0.54 g, 1.0 mmol) instead of PNP. Yield 90%. Anal. Calcd for $C_{42}H_{55}IrN_2P_2$: C, 59.91; H, 6.58; N, 3.33; Ir, 22.83. Found: C, 59.84; H, 6.62; N, 3.13; Ir, 22.51. The presence of formaldehyde in the reaction mixture was determined as described above.

Preparation of $[(PNP)Ir(\eta^4\text{-cod})]BPh_4$ (5). Solid PNP (0.48 g, 1.0 mmol) was added with stirring to a solution of $[Ir(cod)Cl]_2$ (0.34 g, 0.5 mmol) in THF (20 mL) at room temperature. Addition of $NaBPh_4$ (0.60 g, 1.75 mmol) in ethanol (30 mL) and slow evaporation of the solvent gave yellow crystals of **5**. Yield 95%. Λ_M = 56 Ω^{-1} cm^2 mol^{-1}. Anal. Calcd for $C_{63}H_{67}BIrNP_2$: C, 68.59; H, 6.12; N, 1.27; Ir, 17.42. Found: C, 68.41; H, 6.16; N, 1.18; Ir, 17.22.

Preparation of $[(P_2N_2)Ir(\eta^4\text{-cod})]BPh_4$ (6). Compound **6** was prepared as described above for **5** by using P_2N_2 (0.54 g, 1.0 mmol) instead of PNP. Yield 95%. Λ_M = 54 Ω^{-1} cm^2 mol^{-1}. Anal. Calcd for $C_{66}H_{74}BIrN_2P_2$: C, 68.32; H, 6.43; N, 2.41; Ir, 16.57. Found: C, 68.07; H, 6.40; N, 2.38; Ir, 16.24.

Reaction of 5 and 6 with $LiHBEt_3$. $LiHBEt_3$ (1 M in THF, 0.5 mL, 0.5 mmol) was syringed into a stirred solution of **5** (0.55 g, 0.5 mmol) [or of **6** (0.58 g, 0.5 mmol)] in THF (20 mL) at room temperature. On addition of ethanol (20 mL) and partial evaporation of the solvent, crystals of **1** (or **2**) precipitated in 85% yield.

Preparation of $[(triphos)Ir(\sigma,\eta^2\text{-}C_8H_{13})]$ (7). Solid triphos (0.62 g, 1.0 mmol) was added with stirring to a solution of $[Ir(cod)OMe)]_2$ (0.33 g, 0.50 mmol) in THF (30 mL). On addition of ethanol (30 mL) and partial evaporation of the solvent, yellow crystals of **7** precipitated in 95% yield. The presence of HCHO in the reaction mixture was determined

(4) (a) *Homogeneous Catalysis with Metal Phosphine Complexes*, Pignolet, L. H., Ed.; Plenum Press: New York, 1983, p 257. (b) Catalytic Aspects of Metal Phosphine Complexes, Alyea, E. C., Meek, D. W., Eds. *Adv. Chem. Ser.* **1982**, 196. (c) DuBois, D. L.; Meek, D. W. *Inorg. Chim. Acta* **1876**, *19*, L29. (d) Bianchini, C.; Mealli, C.; Meli, A.; Peruzzini, M.; Zanobini, F. *J. Am. Chem. Soc.* **1988**, *110*, 8725. (e) Bianchini, C.; Meli, A.; Peruzzini, M.; Vizza, F.; Frediani, P.; Ramirez, J. A. *Organometallics* **1990**, *9*, 226.

(5) Sacconi, L.; Morassi, R. *J. Chem. Soc. A* **1969**, 2904.

(6) (a) Sacconi, L.; Morassi, R. *J. Chem. Soc. A* **1971**, 492. (b) Di Vaira, M.; Midollini, S.; Sacconi, L. *Inorg. Chem.* **1978**, *17*, 816.

(7) Bianchi, A.; Dapporto, P.; Fallani, G.; Ghilardi, C. A.; Sacconi, L. *J. Chem. Soc., Dalton Trans.* **1973**, 1973.

(8) Morassi, R.; Bertini, I.; Sacconi, L. *Coord. Chem. Rev.* **1973**, *11*, 343.

(9) Farnetti, E.; Kaspar, J.; Spogliarich, R.; Graziani, M. *J. Chem. Soc., Dalton Trans.* **1988**, 947.

(10) Giordano, G.; Crabtree, D. H. *Inorg. Synth.* **1979**, *19*, 218.

(11) Hewertson, W.; Watson, H. R. *J. Chem. Soc.* **1962**, 1490.

(12) Casciellano, S.; Bothner-By, A. A. *J. Chem. Phys.* **1964**, *41*, 3863.

(13) Gambarotta, S.; Strologo, S.; Floriani, C.; Chiesi-Villa, A.; Guastini, C. *J. Am. Chem. Soc.* **1985**, *107*, 6278.

(14) *International Tables for X-Ray Crystallography*; Kynoch Press: Birmingham, U.K. 1974; Vol. IV.

Table I. Summary of Crystal Data, Data Collection Parameters, and Structure Refinement for **1**

formula	$C_{39}H_{48}NP_2Ir$
M	748.9
cryst syst	monoclinic
space group	$P2_1/c$
a, Å	17.119 (3)
b, Å	9.923 (2)
c, Å	21.289 (4)
β, deg	110.14 (3)
V, Å^3	3395.2
Z	4
D(calcd), g cm^{-3}	1.54
μ(Mo Kα), cm^{-1}	42.8
cryst size, mm	0.15 × 0.25 × 0.50
transmission factors	0.783–0.999
radiation	graphite-monochromated Mo Kα (λ = 0.7107 Å)
scan type	$w/2\theta$
θ range deg	3–28
scan speed, deg min	1–20
scan range, deg	0.7 + 0.35 tan θ
aperture width, mm	1.3 + tan θ
aperture height, mm	4
intensity monitors[a]	3
orientation monitors	4
no. of collected data ($\pm h,k,l$)	8865
no. of unique data with $I > 3\sigma(I)$	5758
final no. of variables	388
R[b]	0.02
R_w[c]	0.031
w	1

[a] Measured after each hour. [b] $R = \sum(||F_o| - |F_c||)/\sum|F_o|$. [c] $R_w = [\sum_w(|F_o| - |F_c|)^2/\sum wFc^2]^{1/2}$.

as previously described. Anal. Calcd for $C_{49}H_{52}IrP_3$: C, 63.55; H, 5.66; N, 2.41; Ir, 20.76. Found: C, 63.42; H, 5.71; N, 2.38; Ir, 20.53.

Preparation of [(triphos)Ir(η^4-cod)]BPh$_4$ (8). Solid triphos (0.62 g, 1.0 mmol) was added with stirring to a solution of $[Ir(cod)Cl]_2$ (0.34 g, 0.5 mmol) in THF (30 mL). The initial red color immediately disappeared to produce a yellow solution from which yellow crystals of **8** separated by addition of $NaBPh_4$ (0.60 g, 1.75 mmol) in ethanol (30 mL). Yield 85%. Λ_M = 56 Ω^{-1} cm^2 mol^{-1}. Anal. Calcd for $C_{73}H_{71}BIrP_3$: C, 70.46; H, 5.75; Ir, 15.45. Found: C, 70.12; H, 5.81; Ir, 15.32.

Reaction of 8 with LiHBEt$_3$. Treatment of **8** (0.44 g, 0.35 mmol) in THF (20 mL) with $LiHBEt_3$ (1 M in THF, 0.35 mL, 0.35 mmol) gave a clear yellow solution from which crystals of the σ-cyclooctenyl complex **7** were obtained in 90% yield by addition of ethanol (20 mL) and slow evaporation of the solvent.

Catalytic Experiments. Catalytic reactions were performed by using the following procedure: The iridium dimer $[Ir(cod)X]_2$ (X = Cl or OMe) was dissolved in the appropriate alcohol (propan-2-ol or cyclopentanol) and to the resulting solution an equimolar amount of PNP or P_2N_2 ligand was added under nitrogen. The solution was heated at 83 °C in propan-2-ol (or at 140 °C in cyclopentanol) for 10 min. After this time, a preheated concentrated solution in the same solvent of the substrate to be reduced was added. When complex **1** or **2** was used as the catalyst precursors, the procedure simply consisted of heating the solutions in propan-2-ol or in cyclopentanol at 83 °C or 140 °C, respectively, and then adding the substrate.

X-ray Data Collection and Structure Determination of 1. Crystals of **1** suitable for X-ray diffraction were obtained by slow addition of ethanol to a concentrated solution in methylene chloride at room temperature. Space group and preliminary cell parameters were obtained by using Weissenberg and precession photographs. Unit cell parameters were refined and the intensity collected on an Enraf-Nonius CAD-4 diffractometer. Crystallographic data of interest are reported in Table I. The intensity was corrected for Lorentz and polarization factors. An empirical absorption correction was applied by using the ψ-scan data for reflections having χ values >80°. The structure was solved by the heavy atom method, which allowed location of the independent iridium atom. All other atoms were located through the combination of structure factor calculations and Fourier syntheses. Non-hydrogen atoms were refined by full-matrix least-squares methods with anisotropic thermal parameters. Hydrogen atoms were included at calculated positions and held fixed during the final cycles of the refinement. Atomic scattering factors and anomalous dispersion terms were taken from the literature.[12] Atomic parameters are listed in Table II. Listings of anisotropic temperature factors, fractional coordinates of hydrogen atoms, and structure factor amplitudes are available as supplementary material.

Results and Discussion

Reactions of [Ir(cod)(OMe)]$_2$ with PNP and P_2N_2. Treatment of $[Ir(cod)(OMe)]_2$ in THF or toluene with 2 equiv of either Pr^n-N(CH$_2$CH$_2$PPh$_2$)$_2$ (PNP) or Et$_2$NCH$_2$CH$_2$N(CH$_2$CH$_2$PPh$_2$)$_2$ (N_2P_2) at room temperature results in the formation of pale yellow solutions from which crystals of [(PNP)Ir(σ,η^2-C_8H_{13})] (**1**) or [(P_2N_2)Ir(σ,η^2-C_8H_{13})] (**2**) precipitate by addition of ethanol, respectively (Scheme I, upper). Both compounds are fairly stable in the solid state and in deoxygenated solutions in which they behave as nonelectrolytes. Formaldehyde forms in the course of the reaction, thus indicating that a β-H elimination reaction from the coordinated methoxy group has occurred.[1] However, the IR spectra contain no ν(Ir–H).

In order to gain insight into the fate of the methoxy hydrogen, an X-ray analysis has been carried out on **1** obtained by slow addition of ethanol to a concentrated solution of CH_2Cl_2.

An ORTEP drawing of the molecular structure of **1** is presented in Figure 1. For clarity, only the first carbon atom of the phenyl groups is labeled. Selected bond lengths and angles are listed in Table III. The structure consists of monomeric units with the

Table II. Positional Parameters and Their Estimated Standard Deviations for Compound **1**[a]

atom	x	y	z	B, Å^2	atom	x	y	z	B, Å^2
Ir	0.76980 (1)	0.41259 (2)	0.36326 (1)	2.332 (3)	C19	0.5825 (3)	0.3449 (5)	0.2208 (2)	2.85 (9)
P1	0.82622 (7)	0.3518 (1)	0.28470 (6)	2.84 (2)	C20	0.5735 (3)	0.4723 (6)	0.1927 (3)	3.9 (1)
P2	0.63958 (7)	0.3275 (1)	0.31066 (6)	2.61 (2)	C21	0.5317 (4)	0.4919 (6)	0.1251 (3)	4.6 (1)
N	0.8007 (2)	0.1855 (4)	0.3971 (2)	2.95 (8)	C22	0.4979 (3)	0.3841 (7)	0.0841 (3)	4.4 (1)
C1	0.9376 (3)	0.3748 (5)	0.2979 (2)	3.2 (1)	C23	0.5052 (3)	0.2572 (6)	0.1110 (3)	4.2 (1)
C2	0.9919 (3)	0.4140 (7)	0.3596 (3)	4.6 (1)	C24	0.5469 (3)	0.2369 (6)	0.1795 (3)	3.7 (1)
C3	1.0761 (4)	0.4288 (9)	0.3709 (3)	5.8 (2)	C25	0.8548 (3)	0.1767 (5)	0.4691 (2)	3.6 (1)
C4	1.1072 (3)	0.4016 (8)	0.3211 (3)	5.7 (2)	C26	0.8798 (4)	0.0370 (6)	0.4986 (3)	4.3 (1)
C5	1.0555 (4)	0.3589 (8)	0.2604 (3)	5.9 (2)	C27	0.9314 (4)	0.0497 (8)	0.5723 (3)	5.8 (2)
C6	0.9707 (3)	0.3440 (7)	0.2486 (3)	4.8 (1)	C28	0.7206 (3)	0.1148 (5)	0.3883 (3)	3.4 (1)
C7	0.7812 (3)	0.4000 (6)	0.1963 (2)	3.29 (9)	C29	0.6518 (3)	0.1427 (5)	0.3231 (3)	3.5 (1)
C8	0.7906 (4)	0.5351 (7)	0.1807 (3)	4.8 (1)	C30	0.8213 (3)	0.1670 (5)	0.2841 (2)	4.1 (1)
C9	0.7536 (4)	0.5800 (8)	0.1148 (3)	6.0 (2)	C31	0.8462 (3)	0.1198 (5)	0.3566 (3)	4.0 (1)
C10	0.7089 (4)	0.4947 (9)	0.0651 (3)	6.1 (2)	C32	0.7800 (3)	0.4905 (5)	0.4594 (2)	3.2 (1)
C11	0.7015 (4)	0.3614 (9)	0.0806 (3)	6.0 (2)	C33	0.8585 (3)	0.5044 (5)	0.4486 (2)	2.97 (9)
C12	0.7373 (4)	0.3144 (7)	0.1458 (3)	4.8 (1)	C34	0.8906 (3)	0.6413 (6)	0.4358 (3)	4.1 (1)
C13	0.5542 (3)	0.3514 (5)	0.3440 (2)	3.08 (9)	C35	0.8395 (4)	0.6869 (6)	0.3598 (3)	5.6 (1)
C14	0.5753 (3)	0.3589 (6)	0.4130 (3)	3.9 (1)	C36	0.7493 (3)	0.6152 (5)	0.3320 (3)	3.6 (1)
C15	0.5139 (4)	0.3663 (6)	0.4423 (3)	4.9 (1)	C37	0.6863 (3)	0.6880 (6)	0.3554 (3)	4.4 (1)
C16	0.4312 (4)	0.3687 (7)	0.4023 (3)	5.3 (1)	C38	0.7123 (4)	0.7241 (7)	0.4271 (3)	5.5 (2)
C17	0.4088 (3)	0.3634 (7)	0.3339 (3)	4.9 (1)	C39	0.7282 (3)	0.6041 (6)	0.4702 (3)	5.2 (1)
C18	0.4703 (3)	0.3541 (6)	0.3047 (3)	3.9 (1)					

[a] Anisotropically refined atoms are given in the form of the isotropic equivalent displacement parameter defined as $^4/_3[a^2B(1,1) + b^2B(2,2) + c^2B(3,3) + ab(\cos\gamma)B(1,2) + ac(\cos\beta)B(1,3) + bc(\cos\alpha)B(2,3)]$.

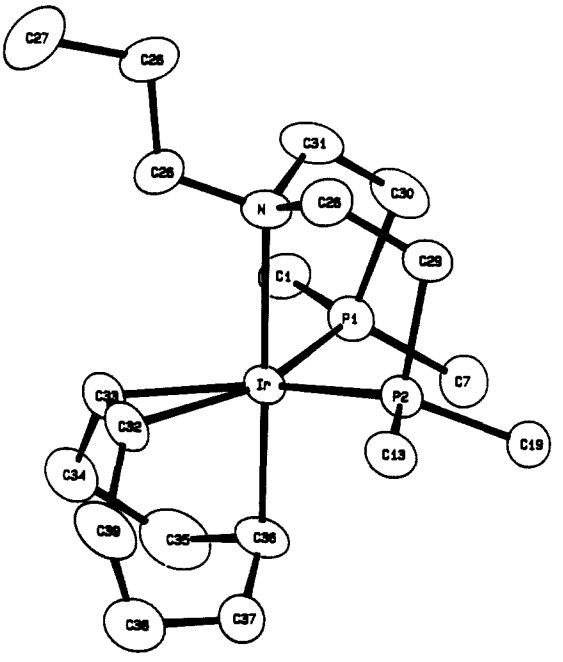

Figure 1. ORTEP diagram of $[(PNP)Ir(\sigma,\eta^2\text{-}C_8H_{13})]$ showing the atom-numbering scheme.

Table III. Selected Bond Lengths (Å) and Angles (deg) with Estimated Standard Deviations in Parentheses for **1**

	(a) Bond Distances		
Ir–P1	2.282 (1)	C32–C39	1.501 (8)
Ir–P2	2.284 (1)	C33–C34	1.525 (7)
Ir–N	2.369 (4)	C34–C35	1.625 (8)
Ir–C32	2.138 (5)	C35–C36	1.588 (8)
Ir–C33	2.129 (4)	C36–C37	1.517 (9)
Ir–C36	2.109 (5)	C37–C38	1.480 (9)
C32–C33	1.444 (7)	C38–C39	1.471 (9)
	(b) Bond Angles		
P1–Ir–P2	97.53 (4)	N–Ir–C32	96.7 (2)
P1–Ir–N	82.3 (1)	N–Ir–C33	97.4 (1)
P1–Ir–C32	151.8 (1)	N–Ir–C36	176.5 (2)
P1–Ir–C33	112.4 (1)	C32–Ir–C36	84.7 (2)
P1–Ir–C36	95.0 (2)	C33–Ir–C36	81.6 (2)
P2–Ir–N	82.86 (9)	C33–C32–C39	125.8 (5)
P2–Ir–C32	110.3 (1)	C32–C33–C34	121.7 (4)
P2–Ir–C33	149.9 (1)	C35–C36–C37	110.9 (4)
P2–Ir–C36	99.7 (1)		

Ir atom coordinated to a cyclooctenyl moiety via σ-C and π-C=C bonding and to the phosphorus and nitrogen donors of the PNP ligand. In particular, it can be observed that metalation has occurred trans to the nitrogen atom. The coordinated polyhedron around the iridium atom can be described as a distorted trigonal bipyramid with nitrogen and C(36) occupying the axial position, with the N–Ir–C(36) angle being 176.5 (2)° (Figure 1). The equatorial plane is defined by two phosphorus atoms and by the olefin, with C(32) and C(33) atoms symmetrically bonded to the iridium atom [Ir–C(32) = 2.138 (5) Å, and Ir–C(33) = 2.129 (4) Å] nearly in the basal plane [Ir, P(1), P(2), C(32), C(33)]. The displacement of the carbon atoms is −0.023 and 0.003 Å, respectively.

In keeping with the crystal structure, the $^{31}P\{^1H\}$ NMR spectrum of **1** in toluene-d_8 at 198 K exhibits an AB spin system with δP_A 13.30, δP_B 10.90 ppm and $J(P_AP_B)$ = 85.5 Hz. Such a pattern is consistent with the nonequivalence of the phosphorus nuclei of PNP as expected because of the different nature of the trans C atoms (one belongs to a five-membered metallaring, the other to a six-membered metallaring). Inspection of the $^{31}P\{^1H\}$ NMR spectra reported in Figure 2 reveals that the temperature not only affects the NMR parameters of **1** but also promotes a reaction. In particular, we note a marked dependence of the chemical shifts of P_A and P_B with the temperature (Figure 3), whereas the J-

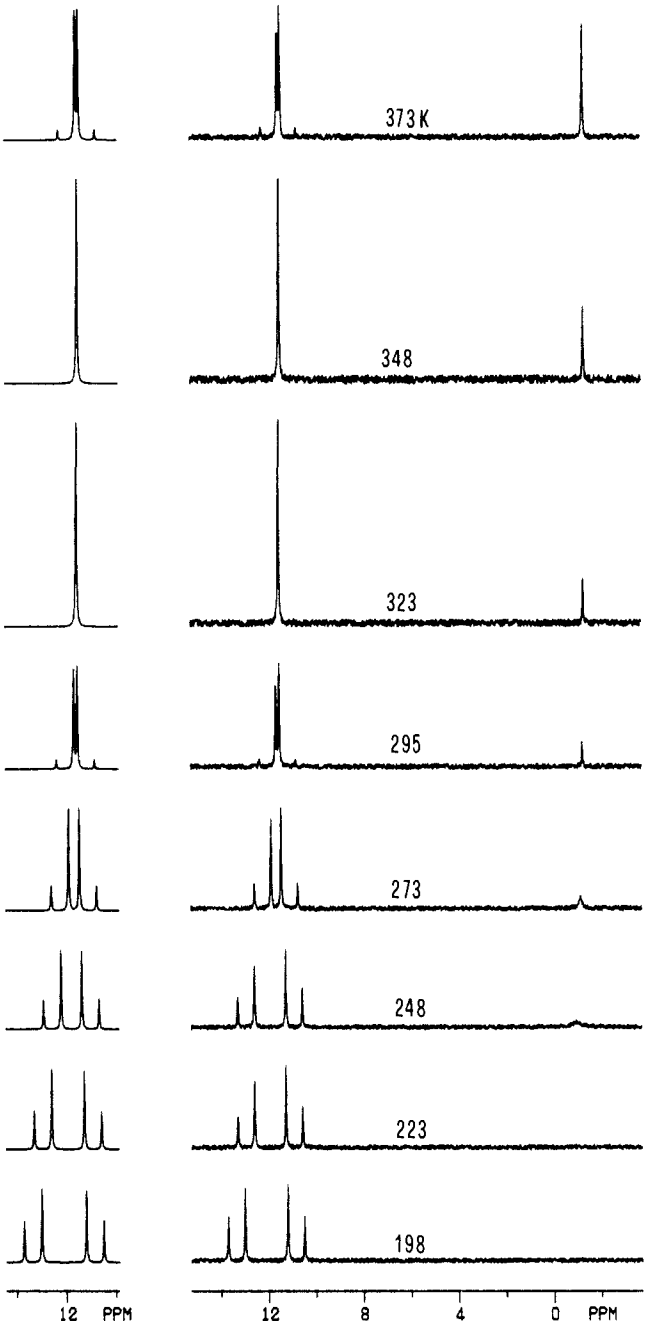

Figure 2. Variable-temperature $^{31}P\{^1H\}$ NMR spectra of a 1:2 mixture of $[Ir(cod)(OMe)]_2$ and PNP in toluene-d_8 (121.42 MHz, 85% H_3PO_4 reference) (right). Computed spectra for the AB spin system of **1** (left).

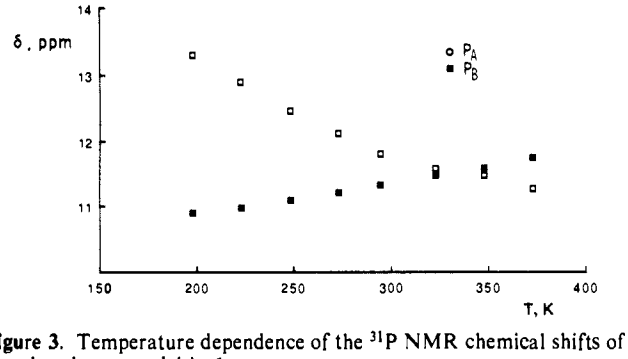

Figure 3. Temperature dependence of the ^{31}P NMR chemical shifts of the phosphorus nuclei in **1**.

(P_AP_B) value remains practically constant. The phenomenon is such that the two chemical shifts concide at ca. 320 K, above which temperature they exchange position. More important and rich of chemical implications is the thermal, reversible transformation

Scheme I

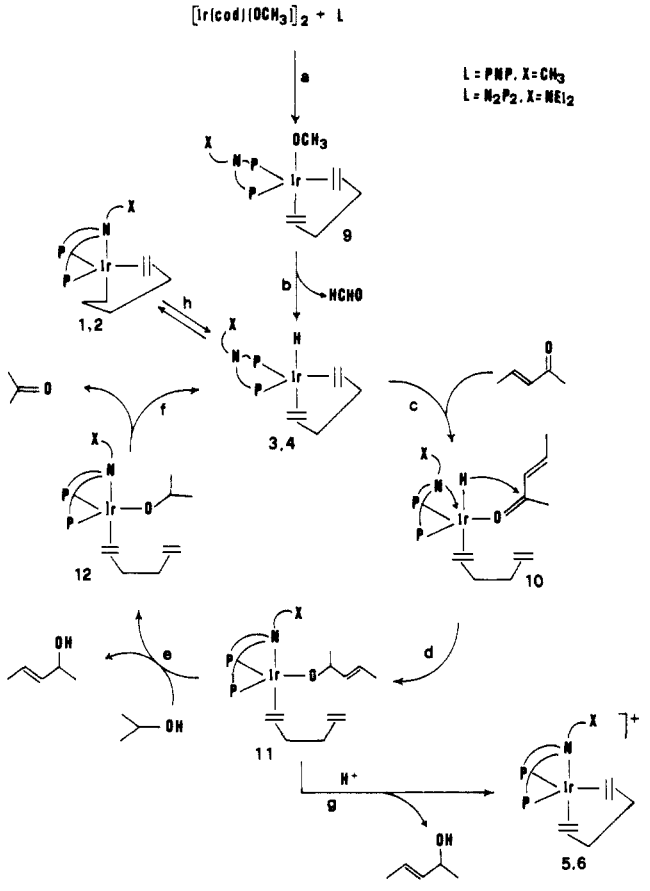

Scheme II

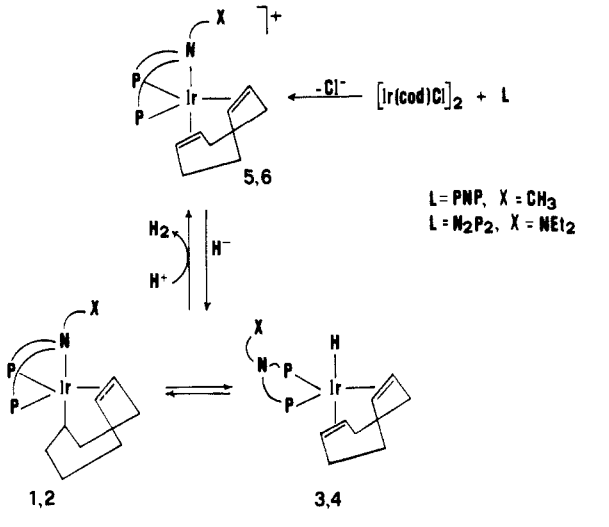

of **1** into a novel species, designated as **3**. An appreciable amount of **3** begins to form at 248 K as shown by the appearance of a singlet at 0.94 ppm. Such an A_2 pattern is consistent with the magnetic equivalence of the two phosphorus nuclei of PNP. On increasing the temperature, the equilibrium concentration of complex **3** increases at the expense of that of **1**. At the highest temperature studied (373 K), a 2.5 ratio between the equilibrium concentrations of **1** and **3** was found (based on NMR integration). Valuable information on the structure of **3** is provided by variable-temperature ^1H NMR spectroscopy in toluene-d_8 solution. At 248 K, the formation of **3** as evidenced by ^{31}P NMR spectroscopy is accompanied by the appearance of a triplet at −13.51 ppm [J(HP) = 21.3 Hz]. The position, the multiplicity, and the value of the coupling constant of this signal are diagnostic for a terminal hydride ligand located cis to two equivalent phosphorus atoms.[15]

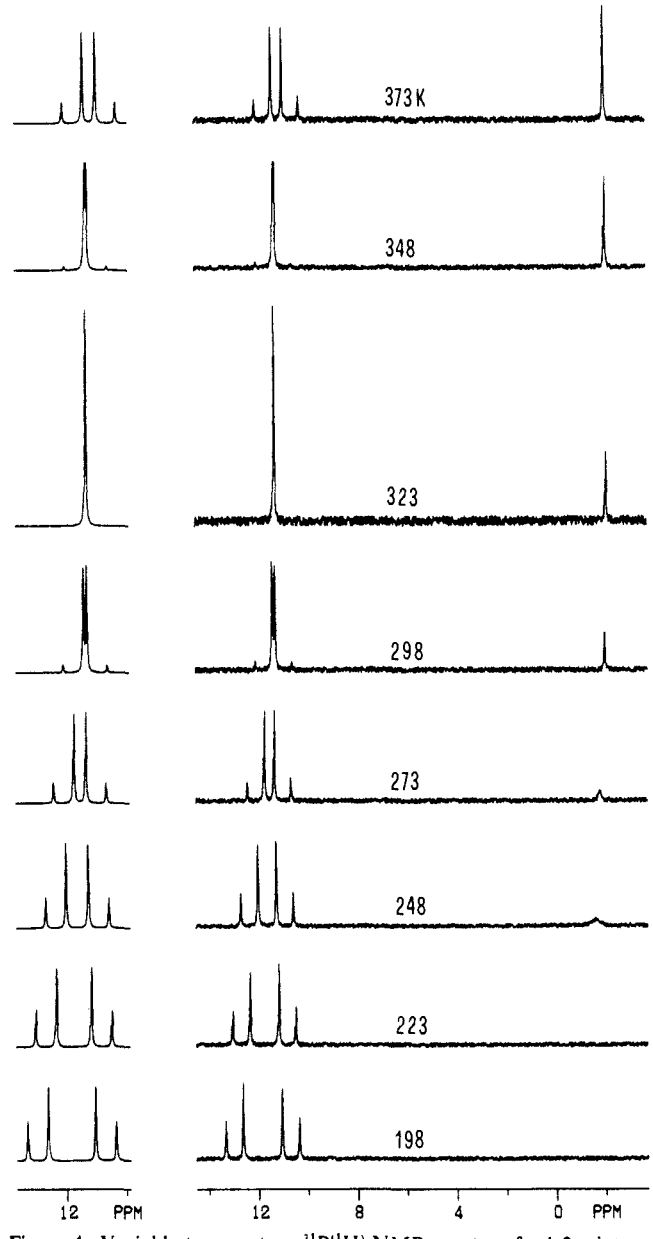

Figure 4. Variable-temperature $^{31}P\{^1H\}$ NMR spectra of a 1:2 mixture of $[Ir(cod)(OMe)]_2$ and P_2N_2 in toluene-d_8 (121.42 MHz, 85% H_3PO_4 reference) (right). Computed spectra for the AB spin system of **2** (left).

The intensity of the triplet increases on increasing the tempeature. Likewise, the ^{31}P NMR AB ↔ A_2 spin system interconversion is reversible, i.e. decreasing the temperature decreases the intensity of the triplet which disappears below 248 K. The triplet at −13.51 ppm is not the only signal to be affected by the temperature as we note also several changes in the 3.7–0.5-ppm region. However, no precise assignment of the resonances can be done due to the large number of protons that resonate in this region. No trace of free cyclooctadiene is detected even at the highest temperature.

In view of the X-ray analysis as well as variable-temperature NMR studies, it is reasonable to conclude that, above 248 K, **1** is in equilibrium with the isomer [(PNP)IrH(η^4-cod)] (**3**) via a β-H elimination/hydride migration process like that shown in the lower part of Scheme II.[16] For several reasons, some of which will be apparent in forthcoming pages, **3** is assigned a structure

(15) (a) Jansen, D.; Venanzi, L. M.; Bachechi, F. *J. Organomet. Chem.* **1985**, *296*, 229. (b) Bianchini, C.; Meli, A.; Peruzzini, M.; Vizza, F.; Frediani, P.; Ramirez, J. A. *Organometallics* **1990**, *9*, 226.

(16) Doherty, N. M.; Bercaw, J. E. *J. Am. Chem. Soc.* **1985**, *107*, 2670. (b) Bunting, H. E.; Green, M. H. L.; Newman, P. A. *J. Chem. Soc., Dalton Trans.* **1988**, 557. (c) McNally, J. P.; Cooper, N. J. *Organometallics* **1988**, *7*, 1704.

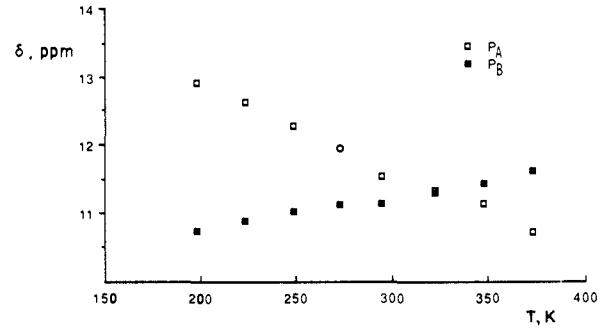

Figure 5. Temperature dependence of the ^{31}P NMR chemical shifts of the phosphorus nuclei in **2**.

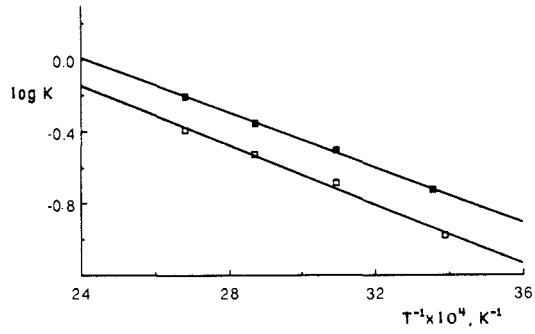

Figure 6. Temperature dependence of the equilibrium constants relative to the **1** ⇄ **3** (□) and **2** ⇄ **4** (■) interconversions.

where PNP behaves as a bidentate ligand through the phosphorus donors. A hydride ligand and a tetrahapto-bonded cycloocta-1,5-diene molecule complete the coordination polyhedron.

A quite similar physical-chemical behavior is exhibited by P_2N_2 complex **2** (Figure 4 and 5 and Scheme I), the only difference being a thermodynamically easier conversion of the σ-cyclooctenyl complex into the hydride (η^4-cycloocta-1,5-diene) derivative $[(P_2N_2)IrH((\eta^4\text{-cod})]$ (**4**). The $^{31}P\{^1H\}$ parameters for compounds **2** and **4** at 298 K in toluene-d_8 are as follows: **2**, AB spin system, δP_A 11.74, δP_B 10.94 ppm, $J(P_AP_B)$ = 82.8 Hz; **4**, A_2 spin system, δP −2.00 ppm. The resonance due to the terminal hydride ligand in **4** becomes evident at ca. 233 K as a triplet centered at −13.43 ppm with $J(HP)$ = 20.9 Hz. Like the analogous resonance in the ^1H NMR spectrum of **3**, the chemical shift of the triplet exhibits a slight temperature dependence (at 348 K δ − 13.70 ppm).

The equilibrium constants for the **1** ⇄ **3** and **2** ⇄ **4** interconversions have been calculated at different temperatures by ^{31}P NMR integration in the temperature range 298–348 K where the equilibrium concentrations of all the species are significant. The log K values have been plotted against $1/T$ giving a satisfactory linear least-squares fit in both cases (the linear correlation coefficients are better than 0.99) (Figure 6). The interpolating functions ($\log K = 1.834 - 825T^{-1}$ and $\log K = 1.831 - 760T^{-1}$, respectively) allow one to calculate the enthalpy and entropy values for the **1** → **3** and **2** → **4** isomerization reactions. The thermodynamic functions for the two conversions are rather similar with each other indicating a reaction mechanism of the same type. This suggests that the terminal NEt_2 group in the P_2N_2 complexes does not participate in the isomerization process. In other words, the terminal nitrogen donor does not seem to coordinate iridium at any stage of the reaction. Accordingly, complex **2** can be reasonably assigned a primary structure quite similar to that experimentally determined for **1**.

From a perusal of the thermodynamic data shown in Table IV, one may readily observe the following: (i) The **1** → **3** and **2** → **4** isomerization reactions are endothermic, thus indicating that the cleavage of the N–Ir bond and the β-H elimination reaction are not energetically compensated by the formation of Ir—H and Ir—(π-C=C) bonds. (ii) The enthalpy contribution is a little bit more favorable for the **2** → **4** conversion. This is in accord with the observed higher concentration of the hydride species for the P_2N_2 system. (iii) The $\Delta S°$ values are positive and consistent with a less rigid conformation of the hydride species as compared to the σ-cyclooctenyl precursors.

Table IV. Thermodynamic Functions for the β-H Elimination Reactions **1** → **3** and **2** → **4**[a]

reaction	$\Delta G°$(298 K), kcal mol^{-1}	$\Delta H°$, kcal mol^{-1}	$\Delta S°$, cal K^{-1} mol^{-1}
1 → **3**	1.27	3.8 (2)	8.4 (7)
2 → **4**	0.98	3.5 (1)	8.4 (3)

[a] Values in parentheses are estimated standard deviations on the last significant figure.

Reactions of $[Ir(cod)Cl]_2$ with PNP and P_2N_2. In order to definitely establish the role played by the methoxy ligand in the formation of **1** and **2**, the two hybrid ligands PNP and P_2N_2 have been reacted with $[Ir(cod)Cl]_2$ under the conditions employed for $[Ir(cod)(OMe)]_2$. As a result, the η^4-cycloocta-1,5-diene complexes $[(PNP)Ir(\eta^4\text{-cod})]BPh_4$ (**5**) and $[(P_2N_2)Ir(\eta^4\text{-cod})]BPh_4$ (**6**) have been quantitatively obtained as yellow crytals by addition of $NaBPh_4$ (Scheme II). The latter counteranion has been used just to improve the crystallization process. Indeed, monitoring the reactions between $[Ir(cod)Cl]_2$ and L by variable-temperature ^{31}P NMR spectroscopy shows that the complex cations $[(L)Ir(\eta^4\text{-cod})]^+$ are both the kinetic and thermodynamic products in the temperature range 333–183 K (L = PNP, N_2P_2).

Compounds **5** and **6** are air-stable in both the solid state and solution where they behave as 1:1 electrolytes. Thermal decomposition of both compounds in the GC injector at 250 °C produces cycloocta-1,5-diene. The $^{31}P\{^1H\}$ NMR spectra in $CDCl_3$ consist of temperature-invariant A_2 spin systems with δP 16.13 (**5**) and 15.82 ppm (**6**). No resonance in the hydride region is displayed by the ^1H NMR spectra which exhibit three well-resolved multiplets for the olefinic and aliphatic hydrogens of cod: **5**, 3.47 (4 H, CH), 1.77 (4 H, CH_2), and 1.43 ppm (4 H, Ch_2); **6**, 3.60 (4 H, CH), 1.82 (4 H, CH_2), 1.48 ppm (4 H, CH_2).

On the basis of all of these data, **5** and **6** are assigned a structure in which iridium is five-coordinated by cyclooctadiene through the two C=C double bonds and by the PNP donor atom set from either PNP or P_2N_2 (Scheme II).

Reaction of either **5** or **6** in THF with an equimolecular amount of $LiHBEt_3$ quantitatively gives the σ-cyclooctenyl compounds **1** and **2**, thus indirectly demonstrating the correctness of the mechanism leading to the formation of **1** and **2** from the straightforward reaction of $[Ir(cod)(OMe)]_2$ with PNP and P_2N_2, respectively. Such a mechanism therefore involves the cleavage of the dimeric structure of $[Ir(cod)(OCH_3)]_2$ by PNP or P_2N_2 to give mononuclear species containing a terminal methoxy ligand. The latter readily β-eliminates a hydrogen to the metal producing formaldehyde and a terminal hydride ligand.

Reactions of $[Ir(cod)Cl]_2$ with Triphos. According to our mechanistic interpretation, the central nitrogen atom in both PNP and P_2N_2 ligands is supposed to play a determinant role in the interconversion between σ-cyclooctenyl and hydride (η^4-cod) structures. In this respect, the β-H elimination reaction involving the Ir–σ-cyclooctenyl moiety would be made possible just by the easy cleavage of the N–Ir bond. In order to verify the role played by the hard N donor, we have replaced PNP and P_2N_2 with the tripodal ligand $MeC(CH_2PPh_2)_3$, triphos, which contains three strong phosphorus donors. Such a ligand has been purposefully chosen because it may reproduce the bonding mode of PNP and N_2N_2 in complexes **1** and **2**. In fact, the tripodal skeleton invariably forces triphos to occupy three facial sites on the coordination polyhedra.[15-17] By so doing, we have been able to synthesize the complex $[(triphos)Ir(\sigma,\eta^2\text{-}C_8H_{13})]$ (**7**), which differs from **1** and **2** in the chelate ring sizes and in having a phosphorus atom in the place of nitrogen (Scheme III). Interestingly, complex **7** is quite stable even in refluxing THF or toluene solutions, thus providing indirect evidence that the β-H elimination/hydride migration mechanism undergone by **1** and **2** is determined by the

(17) (a) Bianchini, C.; Meli, A.; Laschi, F.; Vacca, A.; Zanello, P. *J. Am. Chem. Soc.* **1988**, *110*, 3913. (b) Bianchini, C.; Meli, A.; Laschi, F.; Vizza, F.; Zanello, P. *Inorg. Chem.* **1989**, *28*, 227.

Scheme III

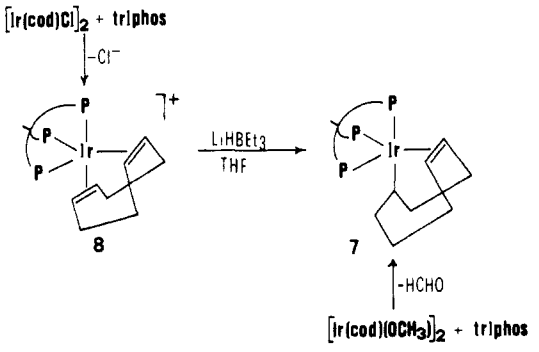

Table V. Reduction of PhCH=CHCOMe to PhCH=CHCH(OH)Me Catalyzed by **1** or **2**[a]

run	catalyst	donor	T, °C	time, min	conv, %	select, %
1	**1**	*i*-PrOH	83	540	41	75
2	**2**	*i*-PrOH	83	540	53	80
3	**1**	CyP-OH	140	90	70	65
4	**2**	CyP-OH	140	10	60	70

[a] [Ir] = 4×10^{-4} M; [sub]/[Ir] = 500; *i*-PrOH = propan-2-ol, CyP-OH = cyclopentanol. % selectivity = (% unsaturated alcohol/% conversion) × 100.

presence of a nitrogen donor in the polydentate ligand.

Compound **7** can be easily prepared as pale yellow crystals by treatment of $[Ir(cod)(OMe)]_2$ in THF with 2 equiv of triphos at room temperature. The compound is air-stable in both the solid state and solution where it behaves as a nonelectrolyte. The presence of formaldehyde as a side product and the absence of ν(Ir–H) in the IR spectrum of **7** are highly diagnostic of σ-cyclooctenyl structure like that found for **1**. Indeed, the compound decomposes in the GC injector at 250 °C producing cyclooctene. The $^{31}P\{^1H\}$ NMR spectrum in $CDCl_3$ shows a temperature invariant AMQ spin system that is consistent with the presence of three different ligands *trans* to the three phosphorus atoms of triphos [δP_A −23.10, δP_M −28.67, δPQ −33.45, $J(P_AP_M)$ = 15.8 Hz, $J(P_AP_Q)$ = 48.3 Hz, $J(P_MP_Q)$ = 18.3 Hz].[2] The ^1H NMR spectrum in $CDCl_3$ is better resolved than those in **1** and **2** and allows one to assign the following resonances to the σ-cyclooctenyl ligand: Ir–CH, multiplet at 2.88 ppm, HC=CH multiplet at 2.62 ppm, $CHCH_2CH$=multiplet at 2.17 ppm, $CHCH_2CH_2$ multiplet at 1.75 ppm, CH_2 (6 H) multiplet at 1.61 ppm.

Alternatively, compound **7** can be prepared by hydride addition to [(triphos)Ir(η^4-cod)]BPh_4 (**8**) which, like the PNP and P_2N_2 congeners, is synthesized by treatment of $[Ir(cod)Cl]_2$ in THF with triphos, followed by $NaBPh_4$ addition (Scheme III). Compound **8** is air-stable in both the solid state and solution where it behaves as a 1:1 electrolyte. The complex is fluxional on the NMR time scale as shown by the $^{31}P\{^1H\}$ NMR spectrum in $CDCl_3$. This consists of a single resonance at −25.29 ppm for the three phosphorus atoms of triphos, exhibiting only a slight temperature dependence of the chemical shift over the range 173–300 K. Such behavior is typical of five-coordinate complexes of triphos and is ascribed to a fast non-bond-breaking interconversion between trigonal-bipyramidal and square-pyramidal structures.[15,17,18] The high fluxionality of **8** is shown by the ^1H NMR spectrum in $CDCl_3$ which displays unique resonances for the four CH hydrogens (3.37 ppm) and the eight CH_2 (2.80 ppm) hydrogens of the η^4-cod ligand.

Catalytic Reduction of PhCH=CHCOMe. The reduction of benzylideneacetone was carried out by using propan-2-ol or cyclopentanol as the donor molecule and two different catalytic systems: isolated compound **1** or **2** was used as the catalyst precursor (system A); the catalyst was prepared in situ mixing equimolecular amounts of $[Ir(cod)(OMe)]_2$ and PNP or P_2N_2 in the appropriate alcohol (system B). The results obtained with

(18) Dahlenburg, L.; Mirzaci, F. *Inorg. Chim. Acta* **1985**, 97, L1.

Table VI. Reduction of PhCH=CHCOMe to PhCH=CHCH(OH)Me Catalyzed by "$[Ir(cod)(OMe)]_2$ + L"[a]

run	L	donor	T, °C	time, min	conv, %	select, %
1	PNP	*i*-PrOH	83	240	90	77
2	P_2N_2	*i*-PrOH	83	120	90	80
3	PNP	CyP-OH	140	30	90	70
4	P_2N_2	CyP-OH	140	2	93	71

[a] [Ir] = 4×10^{-4} M; [L]/[Ir] = 1; [sub]/[Ir] = 500; *i*-PrOH = propan-2-ol, CyP-OH = cyclopentanol.

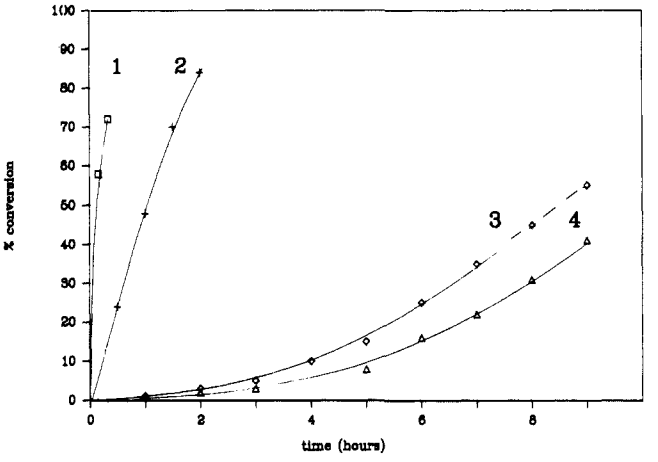

Figure 7. Plot of percent conversion vs time for the hydrogen-transfer reduction of PhCH=CHCOMe catalyzed by **1** (curve 2 in cyclopentanol and 4 in propan-2-ol) and by **2** (curve 1 in cyclopentanol and 2 in propan-2-ol).

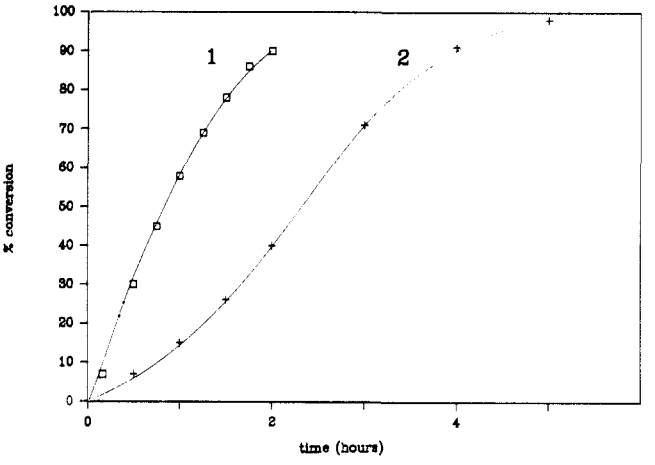

Figure 8. Plot of percent conversion vs time for the hydrogen-transfer reduction of PhCH=CHCOMe catalyzed by the systems "$[Ir(cod)(OMe)]_2$ + P_2N_2" and "$[Ir(cod)(OMe)]_2$ + PNP" prepared in situ (curve 1 and curve 2, respectively).

the two systems are reported in Table V and VI. A perusal of these results reveals that, regardless of the catalytic system, the P_2N_2 catalysts are invariably more active than those with PNP. The data of Table V are also reported in Figure 7 and some interesting conclusions can be drawn. The induction period (curves 3 and 4 of Figure 7), which is present at 83 °C in propan-2-ol, disappears when cyclopentanol is used as the donor molecule and the temperature is raised to 140 °C. Table VI reports the data obtained with use of the catalytic systems prepared in situ. Only the results obtained in propan-2-ol are plotted in Figure 8 since the conversion was difficult to measure in cyclopentanol at 140 °C due to the high catalytic activity of the system at this temperature. Again, P_2N_2 gives rise to a more active system than that formed with PNP, but the selectivities observed with either system A or B are quite similar with each other (compare Tables V and VI). Moreover, the catalytic activities obtained with **1** and **2** as catalyst precursors are invariably lower than those found for the systems prepared in situ. As an example, one can compare

run 1 of Table V and curve 4 of Figure 7 (41% conversion in 540 min and ca. 20% in 240 min) with run 1 of Table VI and curve 2 of Figure 8 (90% conversion in 240 min while 40% conversion is reached in 120 min). Interestingly, the selectivities in unsaturated alcohol are very similar, 75% and 77%, respectively.

These results are consistent with the chemistry in solution of **1** and **2** described in the previous section as well as the reaction path reported in Scheme I. This involves reaction of $[Ir(cod)(OMe)]_2$ with PNP or P_2N_2 [step a] to give five-coordinate intermediate species, $[(L)Ir(\eta^4\text{-cod})(OMe)]$ (L = PNP (**9**), P_2N_2 (**10**)), through the cleavage of the methoxy bridge.[19] Subsequent β-H abstraction from the methoxy ligand readily occurs with formation of equilibrium concentrations of hydrides **3** or **4** and formaldehyde. At this point, we suggest that the unsaturated ketone approaches the complex displacing one olefinic end. The behavior of cyclooctadiene as a monodentate ligand has been previously reported to occur in the platinum compound $[Pt_2(\mu\text{-}SO_2)_2(cod)_2]$, where one of the two molecule of diolefin behaves as a monodentate ligand through an olefinic end.[20] Step d is most likely the key step to the reaction; the selective transfer of hydride to the carbonyl group of coordinated ketone could be promoted by the intramolecular coordination of the free nitrogen donor to form intermediate **11**. Recently, carbon monoxide insertion across the Rh–C bond to give σ-acetyl was reported to be assisted by intramolecular coordination of a dangling phosphine arm of the tripodal polyphosphine PP_3 $[P(CH_2CH_2PPh_2)_3]$ during the carbonylation reaction of $[(PP_3)RhMe]$.[21] Also, the mixed donor ligand $[N(CH_2CH_2PPh_2)_3]$ (NP_3) behaves as a tridentate ligand through phosphorus in the trihydrides $[(NP_3)MH_3]$ (M = Rh and Ir). The rhodium complex is not stable and converts to the monohydride $[Rh(NP_3)H]$ via dihydrogen elimination promoted by intramolecular coordination of the nitrogen donor to the metal.[21] Coming back to Scheme I, the reaction of intemediate **11** with propan-2-ol cleaves the Ir-O bond with consequent formation of free unsaturated alcohol and a σ-isopropoxy complex. Finally step f, which can be considered the reverse of steps c and d, restores the parent hydride via β-H elimination reaction, thereby closing the catalysis cycle.

Interestingly, the reaction of compound **1** or **2** in THF with the unsaturated ketone, followed by addition of an equivalent amount of a protic acid such as $HOSO_2CF_3$, gives quantitative formation of unsaturated alcohol and $[PNP)Ir(\eta^4cod)]^+$ (step g of Scheme I). The result of this reaction is consistent with the formation of an isopropoxy intermediate of type **11** in the catalytic cycle. In this respect, it is noteworthy that, in the absence of a protic acid, **1** and **2** are recovered intact after reaction with benzylideneacetone in refluxing THF.

We have anticipated, when **1** or **2** is employed as catalyst precursors in propan-2-ol at 83 °C, the reactions show an induction period that disappears, or at least becomes very small, when the reactions are carried out at 140 °C in cyclopentanol (Table V and Figure 7). When the catalyst is produced in situ (Table VI and Figure 8), the induction period is much shorter and the catalytic activity is higher than that observed by using isolated **1** or **2**. However, in both cases, the selectivities are very similar to each other (compare the results of Table IV with the corresponding data in Table V). These results can be interpreted on the basis of the solution chemistry of **1** and **2** outlined in the previous sections. The presence of the equilibrium indicated by step h in Scheme I is the main feature of the entire catalytic system. Equilibria **1** $\rightleftarrows$ **3** and **2** $\rightleftarrows$ **4** are shifted to the right (hydride formation) on increasing the temperature and this explains the disappearance of the induction period on going from propan-2-ol to cyclopentanol. Reasonably, the hydride forms during the induction time and then enters into the catalytic cycle. The difference in catalytic activity between **1** and **2** (Table V, runs 1, 2, and 3, 4) is consistent with the thermodynamic data reported in Table IV. From the $^{31}P\{^1H\}$ NMR spectra it is clear that, at comparable temperatures, the equilibrium concentration of the hydride is higher for the P_2N_2 complex that for the PNP analogue (as an example, at 100 °C the concentration ratios **4**/**2** and **3**/**1** are 0.6 and 0.4, respectively). The larger amount of hydrido species in the case of the P_2N_2 complex is in accord with its higher catalytic activity.

The results obtained with the system in situ can be interpreted in a similar way (compare the results in Table VI). The occurrence of β-H elimination/hydride migration equilibria accounts well for the higher activity of the catalysts prepared in situ as compared to isolated **1** and **2**. In fact, after the bridge-splitting reaction between $[Ir(cod)OMe)]_2$ and the PNP and P_2N_2 ligands, the resulting intermediate **9** undergoes β-H abstraction reaction to form straightforward hydrides **3** or **4** that are ready to enter into the catalysis cycle. This explains why the catalytic activity of system B is higher than that obtained with compounds **1** or **2**, while a quite similar selectivity is exhibited.

When the reduction of benzylideneacetone was attempted with the triphos $\sigma,\eta^2\text{-}C_8H_{13}$ complex **7** as the catalyst, we observed a very poor hydrogenation activity giving selectively the saturated ketone. This behavior may be interpreted in terms of the higher donating properties of tertiary phosphines as compared to amines. In other words, unlike the (PNP)Ir and $(P_2N_2)Ir$ systems, the (triphos)Ir fragment is not expected to have any pronounced arm-off process. As a matter of fact, the metallated complex **7** is quite stable in solution where it shows no evidence for β-H elimination reaction leading to Ir–H species. For a similar reaction, i.e. the impossibility of generating a metal hydride complex, the η^4-cod complexes **5**, **6**, and **8** do not exhibit appreciable effectiveness in hydrogen-transfer reduction of α,β-unsaturated ketones.

Acknowledgment. Authors thank "Progetti Finalizzati Chimica Fine e Secondaria" C.N.R., Rome, Italy, for financial support.

Supplementary Material Available: Tables of displacement parameter expressions and positional parameters (4 pages); listing of observed and calculated structure factors (24 pages). Ordering information is given on any current masthead page.

(19) Fernandez, M. J.; Esteruelas, M. A.; Covarrubias, M.; Oro, L. A. *J. Organomet. Chem.* **1986**, *316*, 343.
(20) Farrar, D. H.; Gukathasan, R. R. *J. Chem. Soc., Dalton Trans.* **1989**, 557.
(21) Bianchini, C.; Masi, D.; Meli, A.; Peruzzini, A.; Zanobini, F. *J. Am. Chem. Soc.* **1988**, *110*, 6411.